LEED determination of the structures of Ni(111) and the p(2*2) overlayer of potassium on Ni(111)

1993 J. Phys.: Condens. Matter 5 2875

(http://iopscience.iop.org/0953-8984/5/18/009)

J. Phys.: Condens. Matter 5 (1993) 2875–2886. Printed in the UK

LEED determination of the structures of Ni(111) and the p(2×2) overlayer of potassium on Ni(111)

P Kaukasoina†, M Lindroos†, R D Diehl‡, D Fisher§‖, S Chandavarkar§¶ and I R Collins§††

† Department of Physics, Tampere University of Technology, Tampere, Finland
‡ Department of Physics, Penn State University, University Park, PA 16802, USA
§ Department of Physics and Surface Science Centre, University of Liverpool, Liverpool L69 3BX, UK

Received 14 December 1992

Abstract. We have used dynamical low-energy electron diffraction (LEED) to determine the structure of both the clean Ni(111) surface and the p(2×2) structure of potassium adsorbed on Ni(111). The result of the clean surface study indicates that the Ni(111) is essentially a truncation of the bulk crystal. The p(2×2) structure of potassium on this surface consists of the potassium atoms adsorbed on top of the Ni atoms with a slight reconstruction of the top-layer Ni atoms combined with vertical relaxations of the first and second layers of Ni. The potassium–nickel bond length is 2.82±0.04 Å corresponding to an effective potassium radius of about 1.57 Å. This result fits well in the bond length versus coordination number trend observed for other alkali metal overlayers.

1. Introduction

In the past two years a great many surprises have occurred in the study of the structures of alkali metal adsorbates on metal surfaces. Until these studies, the main point of interest in alkali metal adsorption on flat metal surfaces was the nature of the chemisorption bond at low coverages, which was variously interpreted as being ionic or covalent [1,2]. Even though a relatively early LEED study of Cs on Cu(111) indicated that Cs occupied sites on top of Cu atoms [3], alkali metal adsorbates were generally expected to adsorb in the hollow sites on metal surfaces because it was thought that their simple electronic arrangement should favour high-coordination sites. They were also expected to remain on top of the surface, and not to diffuse into or mix with metal surfaces because of their low bulk solubilities. Recent experiments however, show that adsorption in low-coordination sites appears to be the rule rather than the exception on close-packed substrates [4–8]. Vacancy site adsorption (also called substitutional adsorption) in which the adsorbate atom has a coordination number of six has also been observed [7,9]. In fact, complete intermixing of adsorbate and substrate has been observed, including cases of ordered bilayers of mixed alkali metal atoms and

‖ Present address: DTC, Maidenhead, Berks, UK.

¶ Present address: FOM Institute for Atomic and Molecular Physics, Amsterdam, The Netherlands.

†† Present address: Institut de Physique Appliquée, Ecole Polytechnic Fédérale (Ecublens), CH-1015, Lausanne, Switzerland.

0953-8984/93/182875+12$07.50

substrate atoms [10]. Table 1 lists the experimentally determined structural parameters of submonolayers of adsorbed alkali metals on simple metal surfaces.

Some of the experimental results described in this paper have been reported in a previous letter [4] and the purpose of this paper is to present the complete set of LEED results for the clean Ni(111) surface along with a more detailed analysis of the p(2×2) overlayer of K on Ni(111), and to provide a brief summary of the structural determinations for alkali metal adsorbates, particularly with respect to their adsorption sites and chemisorption bondlengths.

2. Experiment

The experiments were carried out in an ultra-high vacuum system which was mu-metal shielded and had a base pressure of 6×10^{-11} mbar. The data was obtained using a standard Varian 4-grid optics in constant-beam-current mode and a video data acquisition system [11]. Briefly, the video data acquisition system consisted of a Sony CCD video camera and a Data Translation frame grabber board in a Micro Vax computer which was situated near the experiment. Image analysis was accomplished by a combination of Data Translation and custom-written software. The crystal was cut to within 0.25° of the (111) surface and was subsequently mechanically polished and chemically etched. It had been used in adsorption studies for at least two years prior to this experiment and so had been through many cycles of 0.5 keV Ar^+ ion bombardment and annealing to 1200 K. After additional cleaning cycles before running each of these experiments, the crystal was heated to 1200 K and slowly cooled at a rate of about 1 K s^{-1} to 120 K. The purpose of the slow cooling rate was to minimize the step density on the surface, thereby creating larger 'perfect' terraces for adsorption [21].

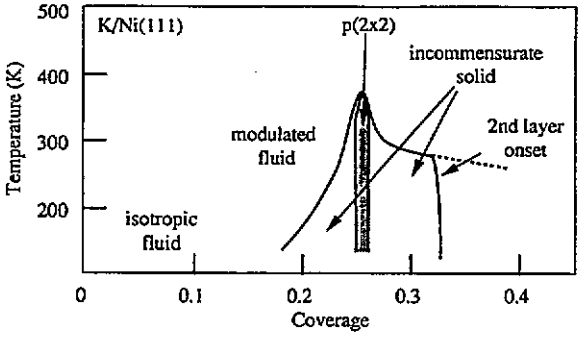

Figure 1. The temperature–coverage phase diagram for the submonolayer potassium on Ni(111).

The phase diagram for K/Ni(111) and the procedure for producing the p(2×2) potassium overlayer were determined in previous LEED experiments [11, 13]. The phase diagram, shown in figure 1, indicates that the potassium overlayer forms either a fluid or a hexagonal incommensurate structure over most of the submonolayer coverage range, except at the coverage of 0.25, where a commensurate p(2×2) structure is formed. The p(2×2) phase is stable to higher temperature than the incommensurate phase at either higher or lower coverages, presumably due to a 'locking in' of the overlayer to the substrate potential. Potassium was evaporated onto the crystal from a SAES getters source which had been

Table 1. Experimentally determined structures for alkali metal adsorption systems. The bondlength quoted is the chemisorption bondlength, effective r is the chemisorption bondlength minus the metallic radius of the substrate atom, excess r is the effective r minus the ionic radius of the alkali metal atom. N is the coordination number of the alkali adatom, and ionic r and metallic r correspond to the ionic and metallic radii respectively of the alkali metal atoms, according to Ashcroft and Mermin [29]. A coordination number is not given for K/Co(10$\bar{1}$0) because the large surface reconstruction complicates the assignment of a coordination number.

System	Structure	Site	Method	Bondlength	Effective r	Excess r	N	Ionic r	Metallic r	Reference
Cs/Rh(100)	c(4×2)	hollow	LEED	3.44	2.10±0.06	0.43	4	1.67	2.73	[30]
Cs/Cu(111)	p(2×2)	top	LEED	3.01	1.73±0.05	0.06	1	1.67	2.73	[3]
Cs/Ru(001)	p(2×2)	top	LEED	3.25±0.08	1.9	0.23	1	1.67	2.73	[5]
Cs/Ru(001)	$\sqrt{3}\times\sqrt{3}$	HCP hollow	LEED	3.52±0.02	2.2	0.53	3	1.67	2.73	[5]
Rb/Al(111)	low cov	top	SXW	3.13±0.10	1.70±0.10	0.22	1	1.48	2.43	[6]
Rb/Al(111)	p(2×2)	top	SXW	3.13±0.10	1.70±0.10	0.22	1	1.48	2.43	[6]
Rb/Al(111)	$\sqrt{3}\times\sqrt{3}$	top	SXW	3.13±0.10	1.70±0.10	0.22	1	1.48	2.43	[6]
K/Ni(111)	p(2×2)	top	LEED	2.82±0.04	1.57±0.04	0.24	1	1.33	2.38	[4]
K/Ni(111)	p(2×2)	top	SEXAFS	2.92±0.02	1.67±0.02	0.34	1	1.33	2.38	[8]
K/Cu(111)	p(2×2)	top	SEXAFS	3.07±0.02	1.79±0.03	0.46	1	1.33	2.38	[8]
K/Co(10$\bar{1}$0)	c(2×2)	hollow	LEED	3.12±0.05	1.87±0.05	0.54	—	1.33	2.38	[31]
K/Al(111)	$\sqrt{3}\times\sqrt{3}$	top	LEED	3.23±0.05	1.80±0.05	0.47	1	1.33	2.38	[7]
K/Al(111)	$\sqrt{3}\times\sqrt{3}$	subst.	LEED	3.58±0.03	2.10±0.03	0.73	6	1.33	2.38	[7]
K/Ni(100)	c(4×2)	hollow	LEED	3.10	1.95	0.62	4	1.33	2.38	[32]
K/Ru(001)	$\sqrt{3}\times\sqrt{3}$	HCP hollow	LEED	3.29±0.05	1.98±0.05	0.65	3	1.33	2.38	[37]
K/Ru(001)	p(2×2)	FCC hollow	LEED	3.25±0.05	1.94±0.05	0.61	3	1.33	2.38	[37]
Na/Al(111)	$\sqrt{3}\times\sqrt{3}$	subst.	SEXAFS	3.31±0.03	1.88±0.03	0.91	6	0.97	1.91	[9]
Na/Al(111)	$\sqrt{3}\times\sqrt{3}$	subst.	SXW	3.10±0.06	1.67±0.06	0.70	6	0.97	1.91	[10]
Na/Ni(100)	c(2×2)	hollow	LEED	2.84	1.59±0.1	0.61	4	0.97	1.91	[33]
Na/Al(100)	c(2×2)	hollow	LEED	2.86	1.43±0.07	0.46	4	0.97	1.91	[34]
Na/Al(100)	c(2×2)	hollow	LEED	2.90±0.09	1.46±0.09	0.49	4	0.97	1.91	[35]
Na/Rh(111)	$\sqrt{3}\times\sqrt{3}$	hollow	LEED	2.8	1.45	0.48	3	0.97	1.91	[36]

degassed at essentially the base pressure of the system for three days. To form the p(2×2) structure, potassium was evaporated onto the crystal to a coverage higher than 0.25 and then gently desorbed at 150 °C until a sharp p(2×2) LEED pattern was obtained. The crystal was then set to normal incidence by adjusting it until the energy variations of intensity in equivalent beams were identical by eye. This was checked later by a more detailed analysis of the intensities.

Frames of the full diffraction pattern were acquired over the energy range $80 \leqslant E \leqslant 450$ eV at 2 eV intervals with appropriate camera lens aperture changes to prevent saturation of the camera. After completing the scans for the potassium-covered surface the crystal was heated to 1200 K to remove the potassium and then cooled slowly back down to 120 K and data was acquired for the clean Ni(111) under the same conditions. Each run required less than one hour for setup and data acquisition time.

Spot intensities were extracted from the video frames by integrating the intensity within a 5×5 pixel box, corresponding to an angular acceptance of about 0.7° and centred on the diffraction spot. The appropriate corrections for aperture changes were applied when necessary. In all, spot intensities were acquired for thirteen nickel beams, consisting of five symmetry-inequivalent beams, and twenty potassium beams, consisting of eight symmetry-inequivalent beams. The intensities for the beams which were symmetry equivalent were averaged in order to reduce the errors due to possible misalignment from normal incidence [14].

3. Computational procedures

Theoretical $I(E)$ spectra were calculated using the program package of Van Hove and Tong [15]. The calculation of the clean Ni spectra were made using the renormalized forward scattering (RFS) method which was presented as an example in [15]. For the adsorbate structure the interlayer scattering was treated using the layer-doubling technique, and the reconstructed nickel layers were treated using the combined space method for composite layers by matrix inversion.

The ion-core scattering potentials were of muffin-tin form and were taken from the tabulated nickel and potassium potential of Moruzzi *et al* [16]. Up to eleven phase shifts were calculated. Phase shifts were temperature corrected using an effective Debye temperature of 440 K for bulk nickel layers and 140 K for the potassium surface layer. Up to fifty-three symmetry-inequivalent beams in symmetrized programs of Van Hove and Tong were used in the plane wave expansion of the wave field between atomic layers. For the purpose of r-factor analysis the real part of the optical potential was treated as a variable and spectra were rigidly shifted in 1 eV steps to obtain the best level of agreement between theory and experiment. The imaginary part of the optical potential was proportional to the cube root of the energy. We made no further attempts to vary non-structural parameters to further improve the level of agreement between theory and experiment as our main aim was to obtain the geometry of the surfaces.

Agreement between theory and experiment was tested by a conventional r-factor analysis. For sensitivity analysis, the Pendry r factor [17] was used. As this r factor is highly sensitive to noise in spectra, the experimental spectra were first filtered by a five-point median filter which removes single spikes. Both experimental and theoretical spectra were smoothed by convolving each data set with a 2 eV wide Lorentzian before carrying out the r-factor analysis [17].

4. Results and discussion

4.1. Clean Ni(111)

Previous LEED studies of the Ni(111) surface at room temperature have been carried out using only three diffracted beams for the analysis [18, 19]. The conclusion of those studies was that the surface layer is contracted slightly or not at all. We have carried out a full LEED $I(E)$ study at 120 K in order to test our procedure before proceeding to the adsorbate structure. The results of our analysis are consistent with the previous studies and we present them here because this study has utilized a much larger database than the previous studies. Figure 2 shows the diffraction data and the calculated spectra for the five symmetry-inequivalent beams. The optimization procedure gave a Debye temperature of 375 K and the optimized real part of the optical potential was 8 eV. Figure 3 shows the r-factor plot for dz_{12}, the interlayer spacing between the first and second Ni layers. From this we deduce that the optimum spacing is 2.03±0.02 Å, which is also the bulk spacing of Ni(111). This result fits well with the general trends observed in surface relaxations for FCC (111) surfaces, for which little or no relaxation of the surface layer is generally expected or observed [20, 21]. An embedded-atom calculation for Ni(111) predicted a contraction of 0.05 Å for this relaxation, which is consistent with the tendency of these calculations to give a somewhat too large relaxation [22].

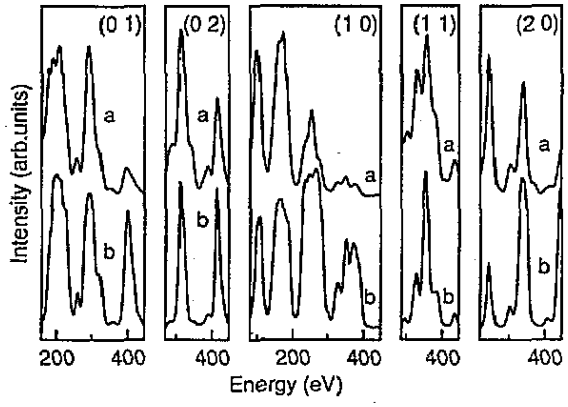

Figure 2. Theoretical (a) and experimental (b) LEED spectra for clean Ni(111).

4.2. K/Ni(111)

The experimental and optimum calculated spectra for thirteen symmetry-inequivalent beams from the p(2×2) structure of potassium on Ni(111) are shown in figure 4. A total of thirty-three beams were measured and averaged to produce these spectra. Five completely different geometries were tested: FCC hollow sites, HCP hollow sites, on-top sites, bridge sites and vacancy occupation of K in the top Ni layer. An initial Pendry r-factor analysis for each structure was carried out, allowing vertical relaxations of the overlayer and substrate. The integer-order beams, which are dominated by scattering from the substrate, were relatively insensitive to the adsorption geometry, while the half-order beams, which are dominated by scattering from the overlayer, are very sensitive to the adsorption geometry. The results of

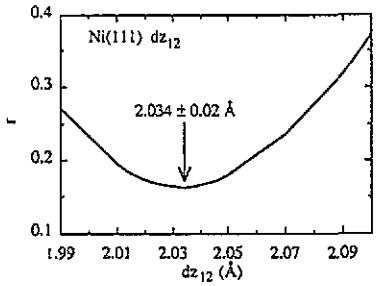

Figure 3. Pendry r factor comparing the experimental data to theoretical data for which the top-layer spacing dz_{12}, of clean Ni(111) is varied. The lowest r factor indicates the best fit.

this preliminary analysis clearly ruled out the hollow sites and the bridge sites on the basis of very poor agreement between theory and experiment for the half-integer beams.

For the top sites and the vacancy-occupation structure we tested more elaborate reconstructions. Two minima were observed for the vacancy occupation, one with a K–Ni vertical distance of 2.71 Å, and one with a K–Ni vertical distance of 0.20 Å. The latter is a truly substitutional structure, with the K atoms almost in the plane of the top Ni layer. The first structure is essentially identical to the best top-site structure, except that there is no Ni atom directly below the K adatom. The best half-integer r factor for this geometry is 0.50, as shown in table 2. The top-site structure had a better half-integer r factor than either of the vacancy-occupation structures. However, because the K–Ni bondlength seemed unusually short in the top-site structure, we looked carefully at the local minima at longer K–Ni bondlengths, including detailed reconstructions. The r factor results of these analyses are shown in table 2. We also considered stacking faults in the Ni near the surface and found poor agreement with the experimental data.

Table 3. r factors of individual beams for the optimum top-site structure.

Integer beams	r factor	Half-integer beams	r factor
(1 0)	0.28	$(\frac{1}{2}\ 0)$	0.33
(0 1)	0.30	$(0\ \frac{1}{2})$	0.32
(1 1)	0.49	$(\frac{1}{2}\ \frac{1}{2})$	0.48
(2 0)	0.15	$(\frac{1}{2}\ 1)$	0.58
(0 2)	0.14	$(1\ \frac{1}{2})$	0.26
		$(\frac{3}{2}\ 0)$	0.30
		$(0\ \frac{3}{2})$	0.55
		$(\frac{3}{2}\ \frac{3}{2})$	0.32

The optimum structure was found to be the top-site structure with a small but significant surface reconstruction in the top two substrate layers. Individual beams r factors are shown in table 3; the structural parameters corresponding to this reconstruction are listed in table 4 and shown in figure 5, and the r-factor plots for some of these parameters are shown in figure 6. The top-layer Ni atoms which are occupied by a K atom have relaxed inward by 0.12 Å relative to those which are not occupied. The atoms in the second substrate layer have smaller vertical relaxations which complement those of the first layer. The unoccupied Ni atoms in the top layer have a small horizontal reconstruction which causes

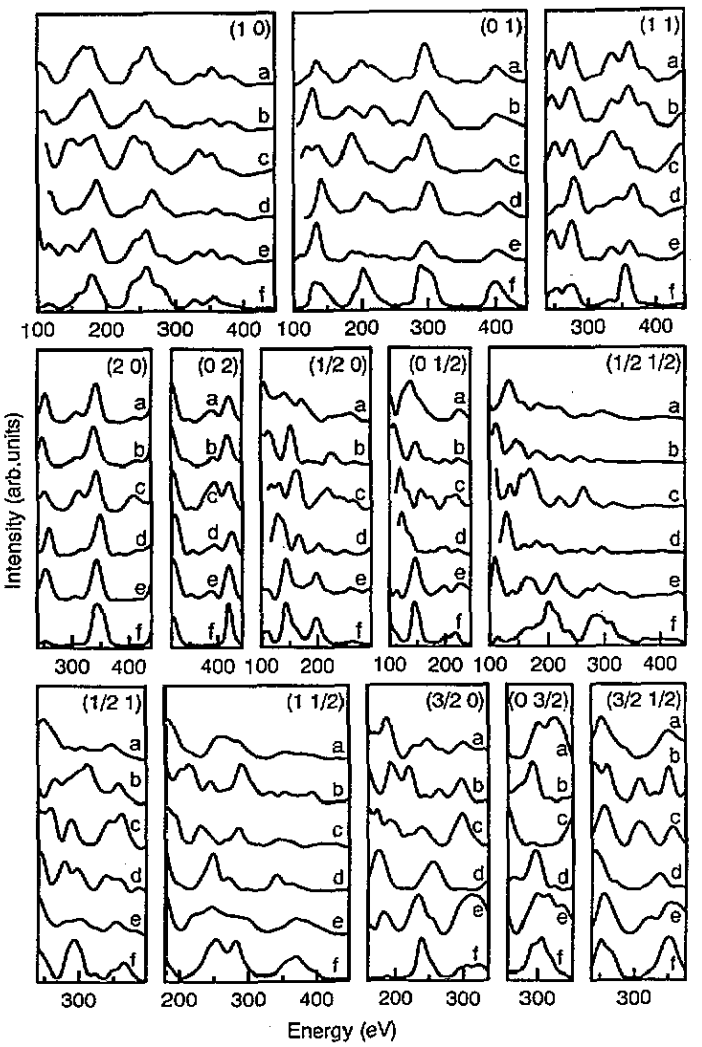

Figure 4. Theoretical (curves a–e) and experimental (curve f) LEED spectra for p(2×2) K on Ni(111). The theoretical spectra have been optimized assuming the following adsorption sites for K: curves a, sixfold vacancy occupation, curves b, bridge site; curves c, HCP hollows; curves d, FCC hollows; curves e, top site.

the unoccupied Ni to draw together in groups of three, away from the K adatoms. The net effect of the substrate reconstruction appears to be to pull the alkali adatom slightly closer to the surface plane than it would be on an unreconstructed substrate. The K–Ni bondlength is 2.82±0.04 Å, which leads to an 'effective radius' of 1.57 Å. The effective radius is simply the difference between the bondlength and the metallic radius of the alkali metal, but it only applies to the adatom–substrate bond. The K radius deduced from the nearest-neighbour K–K spacing in the saturated monolayer is about 2.1 Å [13], indicating that the adatoms are very anisotropic.

The reason for top-site occupation by alkali metals on close-packed metal surfaces is still not well understood. Theoretical attempts to describe it have been limited to the Al(111) substrate [23–25], which is in fact unstable to alkali adsorption and the equilibrium surface

Table 2. Optimum Pendry r factors for different geometries. The first three geometries include vertical relaxations of the substrate. Vacancy and top-site structures have been fully optimized, including substrate reconstructions. The best structure is shown in bold type.

Geometry	Integer beams	Half-integer beams	Overall
K in FCC sites	0.34	0.82	0.63
K in HCP sites	0.47	0.86	0.69
K in bridge site (three domains)	0.32	0.82	0.59
K in vacancy site			
K–Ni = 2.71 Å	0.41	0.50	0.46
K–Ni = 0.20 Å	0.28	0.60	0.43
K on top of Ni			
K–Ni = 2.82 Å	**0.28**	**0.38**	**0.32**
K–Ni = 3.21 Å	0.41	0.51	0.46
K–Ni = 3.61 Å	0.42	0.71	0.56

Table 4. Structural parameters for the optimum top-site structure.

K–Ni nearest-neighbour bondlength	2.82±0.04 Å
K–Ni interlayer spacing	2.70±0.04 Å
Ni first-layer vertical reconstruction	0.12±0.02 Å
Ni dz_{12} interlayer spacing	1.90±0.03 Å
Ni second-layer vertical reconstruction	0.05±0.03 Å
Ni dz_{23} interlayer spacing	2.03±0.04 Å
Ni first-layer horizontal reconstruction	0.06±0.2 Å

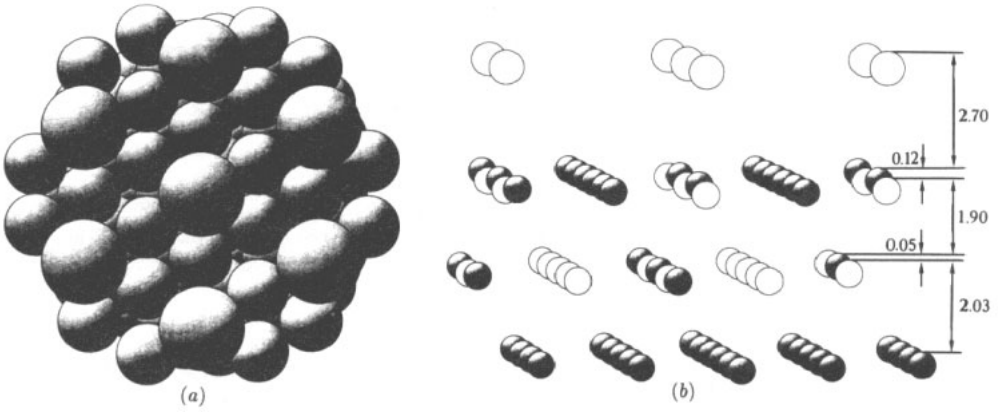

Figure 5. Schematic drawings of the optimum p(2×2) structure: (*a*) view from the top of the crystal showing adatoms in top sites. The radius of the K adatoms is set to be 1.57 Å, the 'effective radius' determined from the chemisorption bondlength (see text). The horizontal reconstruction of the top Ni layer is visible from this view. (*b*) View from the side showing interlayer spacings and vertical reconstructions of the Ni surfaces. The atom sizes are reduced for clarity. Dimensions are in Å.

structures are generally intermixed [6, 7, 9, 10]. It is clear from these calculations though that perhaps the most important component which contributes to top-site occupation is the

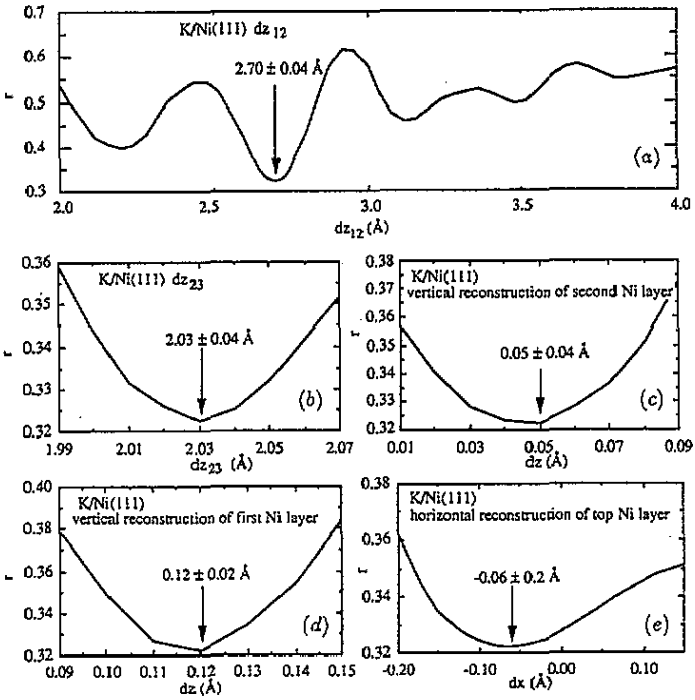

Figure 6. *r*-factor plots for parameters (*a*) dz_{12}, (*b*) dz_{23}, (*c*) vertical reconstruction of top Ni layer, (*d*) vertical reconstruction of second Ni layer, (*e*) horizontal reconstruction of top Ni layer.

almost-flat adsorbate–substrate potential. The flatness of the adsorbate–substrate potential is also evident from the structural studies of these systems which indicate that incommensurate structures dominate their phase diagrams [13, 26]. The preference for the top site then is a rather subtle feature of the adsorbate–substrate interaction. It has been suggested that the preference for top sites is a means of screening the rather large adsorbate–adsorbate repulsion [5], but results of a site determination down to a coverage of 0.12 layers indicate that at least for Rb/Al(111), top sites are still occupied even though the adatoms are spaced far apart [6]. The implication of these results seems to be that when the lateral variation of the repulsive part of the adsorbate–substrate potential is small enough, the attractive part, which is apparently stronger at the top sites due to the higher density of electrons, will dominate. This balance of course could shift with adsorbate coverage since there is a significant change in the details of the charge density as the coverage changes, and indeed a change in site has been observed in the case of Cs/Ru(001), which moves from top to hollow sites as the coverage increases from 0.25 to 0.33 [5].

An interesting feature of the adsorption site differences is the dependence of the adsorbate–substrate bondlength on the adsorption site. Assigning coordination numbers of 1, 3, 4 and 6 to top, threefold hollow, fourfold hollow and sixfold vacancy occupation, respectively, we see in figure 7 a clear dependence of the 'excess radius' on the coordination number. The 'excess radius' is defined as the difference between the effective radius of the alkali metal adatom and its ionic radius. Since the difference between the ionic and metallic radii is very close to 1 Å for all of the alkali metals (see table 1), the excess radius gives a measure of the degree of polarization or ionicity of the adatom.

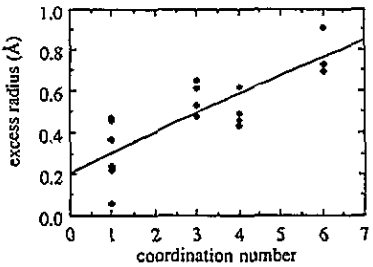

Figure 7. Excess radius (see table 1) of alkali adatoms as a function of coordination number for the systems listed in table 1. The curve is a polynomial fit, but it is meant to be only a guide to the eye.

The general trend of these results is in agreement with the rule of thumb that bondlengths increase with increasing coordination for ionic or covalent bonds, which is also implied by Badger's Rule [27], an empirical relationship which relates the stretching force constants of the individual bonds to their bondlengths. Therefore the change in bondlengths does not imply that there is a qualitative difference in the nature of the bond when the coordination number of the adsorbate changes. It does not rule out qualitative differences, however, and more study is required to elucidate the nature of these bonds.

The substrate reconstructions which accompany these adsorption systems are also very revealing. The degree of reconstruction varies from rather small for most transition metal substrates to massive for aluminium substrates. The effect of the reconstructions in all cases is to increase the coordination of the alkali metal atoms (i.e. increase the number of substrate atoms near the alkali atom). This has been explained for the case of the Al(111) substrate as a means of increasing the screening between the repulsive alkali metal adatoms and thus lowering the total energy of the system [23]. For alkali metals on Al substrates, increasing the temperature from 100 K to room temperature causes a massive reconstruction and intermixing of alkalis to occur [7, 28]. In the case of smaller reconstructions such as for K/Ni(111), it has been observed that there are irreversible quantitative changes in the LEED pattern as the temperature is raised above 100 K which are almost certainly due to a similar but smaller substrate relaxation effect [12, 24]. In other words, the adsorption of an alkali metal on a metal surface can change the surface energy enough to cause a reconstruction or relaxation of the substrate, but the mobility of the substrate atoms at low temperatures might not be great enough to allow the reconstruction or relaxation to occur in a reasonable time. Therefore, the mobility of the substrate atoms is very important to the achievement of equilibrium structures in these adsorption systems. This raises an important point in experimental studies of these overlayers, which is that the temperature history of the overlayer needs to be carefully monitored, because 'annealing' the overlayer to different temperatures may affect the degree of reconstruction and possibly also the chemisorption bondlength. This may explain some of the discrepancies between bondlengths when more than one study was done on the same system. No systematic studies of the chemisorption bondlength on the degree of reconstruction have been made, aside from the large differences observed when the site changes [5, 7].

5. Conclusion

We have shown that the structure of the clean Ni(111) surface is essentially a truncation of

the bulk Ni structure. The equilibrium structure of the p(2×2) potassium overlayer consists of adatoms located on top of Ni atoms and having a K–Ni bondlength of 2.82±0.04 Å. The chemisorption bondlength of alkali metals on metal surfaces generally increases with the coordination number of the adsorption site. Some degree of substrate reconstruction is always present in these systems, the effect of which appears to be to increase the screening between adatoms.

Acknowledgments

We gratefully acknowledge Peter Andrews for the use of his LEED system and Joni Julian for assistance with preparing the figures. We thank C Stampfl for discussions on the LEED analysis. The Isle of Man provided support of DF; PK and ML received support from the National Academy of Finland. Acknowledgment is made to the donors of the Petroleum Research Fund, administered by the ACS, for partial support of this research, and to NSF grant DMR-9022681.

References

[1] Riffe D M, Wertheim G K and Citrin P H 1990 *Phys. Rev. Lett.* **64** 571
[2] Lindgren S Å, Svensson C and Walldén L 1990 *Phys. Rev.* B **42** 1467
[3] Lindgren S Å, Walldén L, Rundgren J, Westrin P and Neve J 1983 *Phys. Rev.* B **28** 6707
[4] Fisher D, Chandavarkar S, Collins I S, Diehl R D, Kaukasoina P and Lindroos M 1992 *Phys. Rev. Lett.* **68** 2768
[5] Over H, Bludau H, Skottke-Klein M, Ertl G, Moritz W and Campbell C T 1992 *Phys. Rev.* B **45** 8638
[6] Kerkar M, Fisher D, Woodruff D P, Jones R G, Diehl R D and Cowie B 1992 *Phys. Rev. Lett.* **68** 3204
[7] Stampfl C, Scheffler M, Over H, Burchhardt J, Nielsen M, Adams D L and Moritz W 1992 *Phys. Rev. Lett.* **69** 1532
[8] Adler D, Collins I R, Ding K, Chandavarkar S, Liang X, Murray S, Leatherman G S, Johnson P D, McGrath R, Diehl R D and Citrin P H to be published.
[9] Schmalz A, Sminpirooz S, Becker L, Haase J, Neugebauer J, Scheffler M, Batchelor D R, Adams D L and Bøgh E 1991 *Phys. Rev. Lett.* **67** 2163
[10] Kerkar M, Fisher D, Woodruff D P, Jones R G, Diehl R D and Cowie B 1992 *Surf. Sci.* **278** 246
[11] Diehl R D and Chandavarkar S 1989 *J. Phys. E: Sci. Instrum.* **22** 651
Chandavarkar S 1989 *PhD Thesis* (University of Liverpool)
[12] Cao Y and Conrad E 1990 *Phys. Rev. Lett.* **65** 2808
[13] Chandavarkar S and Diehl R D 1988 *Phys. Rev.* B **38** 12 112
[14] Davis H L and Noonan J R 1982 **115** L75
[15] Van Hove M A and Tong S Y 1979 *Surface Crystallography by LEED* (Berlin: Springer 1979)
[16] Moruzzi V, Janak J and Williams A 1978 *Calculated Electronic Properties of Metals* (New York: Pergamon)
[17] Pendry J B 1980 *J. Phys. C: Solid State Phys.* **13** 937
[18] Demuth J E, Marcus P M and Jepsen D W 1975 *Phys. Rev.* B **11** 1460
[19] Christman K, Ertl G and Schober O 1973 *Surf. Sci.* **40** 61
[20] Finnis M W and Heine V 1974 *J. Phys. F: Met. Phys.* **4** L37
[21] Van Hove M A, Weinberg W H and Chan C-M 1986 *Low-Energy Electron Diffraction (Springer Series in Surface Sciences 6)* (Berlin: Springer)
[22] Daw M S and Baskes M J 1984 *Phys. Rev.* B **29** 6443
[23] Neugebauer J and Scheffler M 1992 *Phys. Rev.* B **46** 16 067
[24] Annett J F to be published
[25] Guo G-Y to be published
[26] Fan W C and Ignatiev A 1988 *J. Vac. Sci. Technol.* **A6** 735
[27] Badger R M 1934 *J. Chem. Phys.* **2** 128
[28] Andersen J H, Qvarford M, Nyholm R, van Acker J F and Lundgren E 1991 *Phys. Rev. Lett.* **68** 94
[29] Ashcroft N W and Mermin N D 1976 *Solid State Physics* (Philadelphia: Holt, Rinehart and Winston)

[30] Von Eggeling G, Schmidt G, Besold G, Hammer L, Heinz K and Müller K 1989 *Surf. Sci.* **221** 11
[31] Barnes C J, Hu P, Lindroos M and King D A 1991 *Surf. Sci.* **251/252** 561
[32] Bayer U, Oed W, Heinz K and Pendry J B *Surf. Sci.* to be published
[33] Andersson S and Pendry J B 1975 *Solid State Commun.* **16** 563
Demuth J E, Jepsen D W and Marcus P M 1975 *J. Phys. C: Solid State Phys.* **8** L25
[34] Hutchins B A, Rhodin T N and Demuth J E 1976 *Surf. Sci.* **54** 419
[35] Van Hove M A, Tong S Y and Stoner N 1976 *Surf. Sci.* **54** 259
[36] Van Hove M A private communication
[37] Gierer H, Bludau H, Hertel T, Over H, Moritz W and Ertl G 1992 *Surf. Sci. Lett.* **279** L170